Progress In Electromagnetics Research M, Vol. 7, 1–13, 2009

A SIMPLE STRATEGY TO DETECT CHANGES IN THROUGH THE WALL IMAGING

F. Soldovieri

Istituto per il Rilevamento Elettromagnetico dell'Ambiente
Consiglio Nazionale delle Ricerche
Via Diocleziano 328, Napoli 80124, Italy

R. Solimene and R. Pierri

Dipartimento di Ingegneria dell'Informazione
Seconda Univiersita' di Napoli
via Roma 29, Aversa 81031, Italy

Abstract—In this paper, a simple strategy to detect changes in *through-the-wall imaging* scenarios is presented. In particular, tomographic reconstructions taken at different instants of time are exploited. This allows to increase the detectability of scatterers whose positions are varied in two different data collections. The feasibility of the technique is demonstrated with both synthetic and experimental data.

1. INTRODUCTION

The relevance of *through-the-wall imaging* (TWI) techniques is now recognized for the significant applicative advantages that they offer in the rescue assessment and surveillance operations [1, 2] as well as in civil engineering and cultural heritage diagnostics [3].

It is known that TWI is definitely more difficult than free space imaging as it entails dealing with scattering scenarios where the targets are embedded in a complex environment [4]. Accordingly, the frequency band has to be properly selected [5] and the imaging algorithms have to account for the presence of the wall [6–9]. Moreover, in practical situations the wall parameters are unknown or known with

Corresponding author: F. Soldovieri (soldovieri.f@irea.cnr.it).

some degree of uncertainties. Hence, some estimation procedures are also required [7, 10, 11].

Most of the TWI algorithm are concerned with the imaging of stationary targets. Accordingly, information about the geometry of the interior of the building is generally their outcome which is useful, for example, in the design of the rescue operations.

In principle, achieving different images of the same scene according to a temporal frame would allow to image time-varying scene offering the possibility of tracking slowly moving objects like humans. This, of course, requires developing an almost real time imaging procedure (measurement acquisition plus signal processing).

Generally, imaging algorithms [3, 5–11] take few seconds to achieve the images, thus the time to acquire the data is a more critical figure. Indeed, the measurements should be taken *quasi-instantaneously* in order to make negligible the scene's changes during data acquirement otherwise image focusing is deteriorated. To this end, antenna arrays are a more suitable solution than the more usual sliding antenna (which allows to achieve a multimonostatic or multibistatic configurations) but the necessity to keep the number of the antennas minimum and to account for the global response of the system (mutual coupling between the antennas) have to be satisfied.

Developing a target tracking imaging procedure is beyond the scopes of the present paper. Instead, we focus on the possibility of exploiting different data acquisitions to counteract the clutter due to static scatterers present in the scene to be imaged.

To this end, so by accounting that we aim at approaching the problem in realistic cases, we propose a simple procedure based on the *incoherent difference* [12] between two tomographic images of the same scene retrieved at different times.

It is shown, by synthetic and experimental data, that the procedure is capable to highlight changes in the scene allowing for the detection of a scatterer whose position changes in two different data acquisitions and which would be no easily detectable otherwise.

Therefore, the paper is organized as follows. In Section 2, we describe the geometry of the problem and recall the TWI imaging algorithm based on the linear inverse scattering approach [9]. In Section 3, we describe the procedure for static clutter removal. Section 4 is devoted to shown the assessment of the achievable performance by means of synthetic and experimental data. Finally, Conclusions are given.

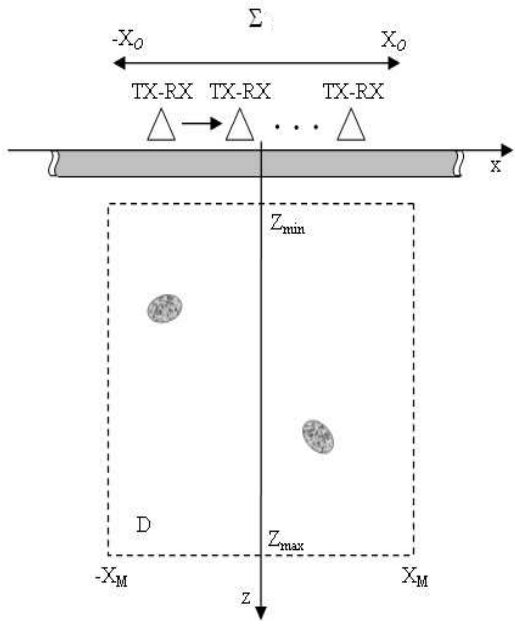

Figure 1. Geometry of the problem.

2. SCATTERING CONFIGURATION AND IMAGING ALGORITHM

We consider the two-dimensional (invariant along the y-axis) scattering configuration depicted in Fig. 1. The targets to be imaged are located within the investigation domain $D = [-x_M, x_M] \times [z_{\min}, z_{\max}]$ hidden behind a wall represented by a slab of thickness d with dielectric permittivity ϵ_b and electric conductivity σ_b. The medium on the opposite sides of the wall is assumed to be free-space whose dielectric permittivity and magnetic permeability are denoted by ϵ_0 and μ_0, respectively. The magnetic permeability of the wall is the one of the free-space.

The electromagnetic parameters of the wall are assumed known [7, 10].

The incident field E_{inc} is provided by a filamentary current directed along y (hence the problem is scalar), located at the air/obstacle interface (see Fig. 1) and radiating within a frequency band $[f_{\min}, f_{\max}]$. The scattered field E_S (i.e., the one due to only the hidden scatterers) is collected at the same position as the source while the latter moves along a rectilinear domain Σ along the x-axis.

In the following, time-dependence $\exp(j2\pi ft)$ is assumed and understood.

According to [9], under the Born approximation [13] the problem of detecting and localizing the scatterers beyond the wall is cast as the inversion of a frequency-domain integral relationship which links the scattered field data E_S to the scatterers represented in terms of the so-called contrast function χ which accounts for the relative difference between the dielectric permittivity of the objects and the ones of the background (free-space) medium

$$E_S(x,f) = k_0^2 \iint_D G\left(x,x',z',f\right) E_{inc}\left(x,x',z',f\right) \times\chi\left(x',z'\right) dx'dz', \tag{1}$$

In Eq. (1), k_0 is free-space wave number and $G(\cdot)$ is the three-layered background medium Green's function [9].

Such a linear inverse problem is solved by resorting to the TSVD inversion scheme [14] which leads to a regularized version of the contrast function $\mathcal{R}\chi$ given by

$$\mathcal{R}\chi = \sum_{n=0}^{N_T} \frac{\langle E_S, v_n\rangle}{\sigma_n} u_n, \tag{2}$$

where N_T is the truncation index, the set $\{\sigma_n\}_{n=0}^{\infty}$ denotes the singular values ordered in a non increasing sequence, whereas $\{u_n\}_{n=0}^{\infty}$ and $\{v_n\}_{n=0}^{\infty}$ form orthonormal bases in the unknown and data spaces, respectively [14].

More details about the imaging algorithm can be found in [9] and in references therein.

3. CHANGE DETECTION TECHNIQUE

In this section, we address the problem of improving the detectability of a target against the clutter due to static scatterers present within the investigation domain D (see Fig. 1). The target is assumed slowly moving in the sense that it is at rest while the aperture is synthesized but its position can change in two different measurement surveys.

The scattered field $E_S(x,f)$ of Eq. (1) can be decomposed as

$$E_S(x,f) = E_{SC}(x,f) + E_{ST}(x,f), \tag{3}$$

where $E_{SC}(x,f)$ denotes the clutter contribution and $E_{ST}(x,f)$ the field due to the object of interest. Consequently, clutter removal

can be cast as the problem of filtering out $E_{SC}(x, f)$ from $E_S(x, f)$. To this end, a filter can be properly designed and tuned on the clutter properties with the constraint of preserving as much as possible $E_{ST}(x, f)$ which is needed for imaging purposes.

In conventional radar systems the so-called moving target indicator (MTI) techniques are designed to detect moving targets against a strong stationary clutter. This is possible because of clutter and targets have different Doppler spectra. Accordingly, a Doppler filtering is designed to cancel the zero Doppler spectral content [15].

A similar filtering is exploited in ground penetrating radar (GPR) imaging [16] where a high-pass filtering suppresses the low harmonic spatial content in order to mitigate the clutter arising from the air/soil interface.

Unfortunately, for the case of concern herein, neither the frequency Doppler shift (as in MTI) nor the difference in the spatial spectral content can be exploited. Indeed, all the scatterers are assumed to be at rest during data acquirement. Moreover, they have all a finite spatial support hence filtering the spatial spectrum as in [16] is not useful.

However, if we could take N different data surveys, that is

$$E_S(x, f, m) \quad m \in (1, 2, \ldots, N), \tag{4}$$

a similar filtering as in [16] can be applied if data are Fourier transformed with respect to the discrete variable m.

Here, we adopt a different procedure where the change detection is achieved by means of the difference between two different tomographic reconstructions of the same spatial region.

Removing clutter by means of a difference procedure has been already documented in the literature. In [12] and [17], the coherent and incoherent difference between two images is exploited, respectively. However, in both papers one of the two images refers to the case where the scatterer of interest is not present. This substantially corresponds to exploiting the background measurement which is difficult to obtain in practical TWI scenarios.

In order to relax the need of the reference image, here the following procedure is exploited.

Say $\mathcal{R}\chi_m(x', z')$ the tomographic reconstruction obtained by processing the data collected at the m-th instant. Then, we consider

$$\left|\mathcal{R}\chi_m\left(x', z'\right)\right| - \left|\mathcal{R}\chi_{m-1}\left(x', z'\right)\right| \tag{5}$$

as the *difference* image at the m-th instant of time, with $|\cdot|$ being the modulus of its argument. In other words, the reconstruction at

the m-th instant of time is obtained by subtracting pixel by pixel the the modulus of the tomographic reconstructions obtained by exploiting $E_S(x, f, m)$ and $E_S(x, f, m-1)$, respectively. The resulting *difference* image is then positively thresholded. This allows to image the targets at the position it was occupying while the m-th survey was being performed. In fact, the difference sign in Eq. (5) will roughly[†] cancel the reconstruction of static scatterers whereas the reconstruction of the target at time $m-1$ will appear under the negative sign and it is then erased by the positive threshold.

This explains why we chose to achieve clutter mitigation in the image domain rather than in data domain. In fact, by inverting $E_S(x, f, m) - E_S(x, f, m-1) = E_{ST}(x, f, m) - E_{ST}(x, f, m-1)$ (which corresponds to the coherent difference in the image domain) would allow a better clutter cancellation (see footnote) but we would be not able to discern the actual target position. The same arguments apply if a filtering procedure is adopted after Fourier transforming with respect to m several data acquisitions.

Of course, if the target does not change its position during two different surveys the proposed procedure will provide a "null image" because also the target itself will be erased in the *difference* reconstruction.

4. RECONSTRUCTION RESULTS

In this section, we show some reconstruction examples to check the effectiveness of the proposed imaging procedure. Both the case of synthetic and experimental data are considered.

4.1. Synthetic Data

The following synthetic examples are obtained by considering a scattering configuration whose parameters are reported in Table 1.

The data are synthesized in time domain thanks to the free code GPRMAX based on a FDTD method [18] and then Fourier transformed in the frequency domain. Finally, the reconstructions are obtained according to Eq. (2) where the singular values above 0.2 times the maximum one are retained.

The clutter scenario consists of two square scatterers having side equal to 0.2 m whose centers are at $(-0.4, 0.9)$ m and $(0.3, 1.1)$ m,

[†] It must be said that due to the nonlinearity of the modulus function the reconstruction of static scatterers is in general different for each measurements survey as they do not sum incoherently to the ones of the targets.

respectively. The shallower square has a dielectric permittivity of $4\epsilon_0$ whereas the other one of $9\epsilon_0$.

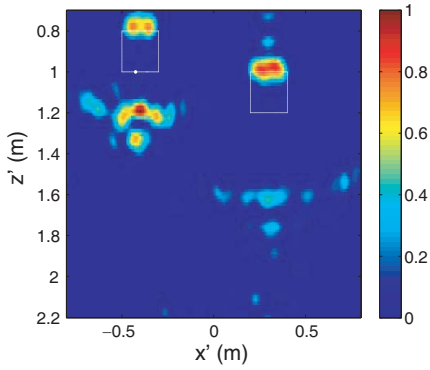

Figure 2. Normalized amplitude reconstruction of the static scatterers. White squares denote actual scatterers.

The corresponding reconstruction is reported in Fig. 2. As can be seen, both the upper and lower edges of the objects are clearly detected and localized. However, as the electromagnetic velocity within the square objects are different from the one assumed in the Born model, the lower edges are not in their actual positions but are delocalized as they appear more deeply located.

Now, as a target to be detected within the above depicted scenario, we consider a circular object of radius equal to 0.1 m and dielectric

Table 1. Parameters of the configuration.

Wall dielectric permittivity ϵ_b	$4\epsilon_0$
Wall conductivity σ_b	$0.05\,\mathrm{S/m}$
Wall thickness d	$0.24\,\mathrm{m}$
Investigation domain D	$[-0.8, 0.8] \times [0.7, 2.2]\,\mathrm{m}^2$
Σ	$[-0.8, 0.8]\,\mathrm{m}$
Spatial step of measurements	$0.04\,\mathrm{m}$
Frequency band	$[1, 2.5]\,\mathrm{GHz}$
Frequency step	$50\,\mathrm{MHz}$
Offset TX-RX	$0\,\mathrm{m}$

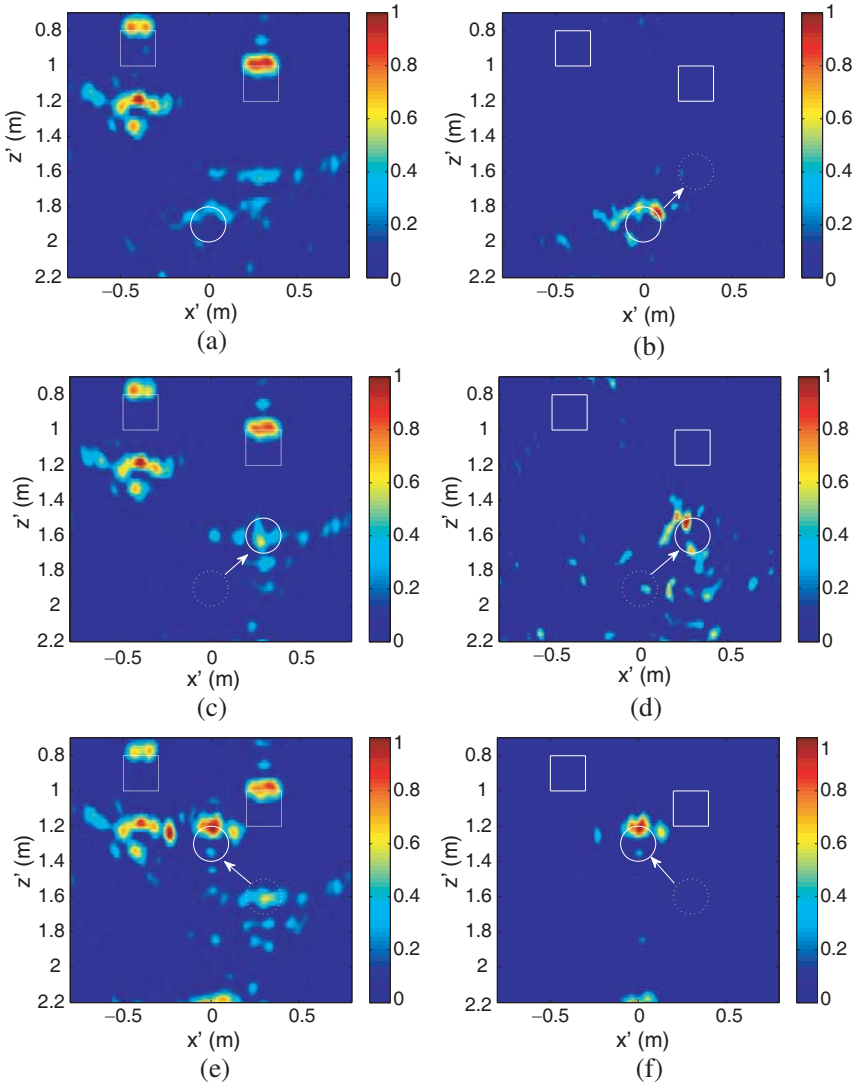

Figure 3. Normalized TSVD tomographic reconstructions and outcomes of the change detection procedure. (a) $|\mathcal{R}\chi_1|$. (b) $|\mathcal{R}\chi_1| - |\mathcal{R}\chi_2|$. (c) $|\mathcal{R}\chi_2|$. (d) $|\mathcal{R}\chi_2| - |\mathcal{R}\chi_1|$. (e) $|\mathcal{R}\chi_3|$. (f) $|\mathcal{R}\chi_3| - |\mathcal{R}\chi_2|$. White solid lines denote scatterers actually present at the considered instant of time. Dotted lines denote scatterers present at the instant of time different from the considered one.

permittivity $20\epsilon_0$. During each single data collection the target is at rest while its position can change in two different data collection.

In particular, we consider the following situations:

$m = 1$, the target center is at $(0, 1.9)$ m

$m = 2$ the target center is at $(0.3, 1.6)$ m

$m = 3$, the target center is at $(0, 1.3)$ m.

The tomographic reconstructions for such scatterer configurations and the corresponding results obtained by the *difference* procedure are reported in Fig. 3.

By comparing panels (a) and (b), panels (c) and (d) and panels (e) and (f) of Fig. 3, it is evident that the proposed procedure allows to increase the detectability of the circular scatterer. Of particular interest is the case reported in panel (d) where the change detection procedure allows to discern the target which is overwhelmed by the reconstruction of deeper side of the square object in front of it (see panel (c)). In panel (d), the circular target is already well visible. However, the change detection procedure allows to better identify the scatterer against the artifacts due to the static square objects.

Similar results (here not reported for brevity) have been also obtained for the more complex background scenario resembling the room of a building addressed in [19].

4.2. Experimental Data

We now turn to show some reconstruction examples obtained by experimental data.

A portable continuous wave stepped frequency radar system working in the frequency band of 800 MHz–4 GHz is employed to collect

Figure 4. Pictorial view of the scene.

the data. Furthermore, two rectangular ridged horn antennas working in the frequency band 800 MHz–5 GHz linearly polarized along y are automatically positioned thanks to a slide driven by a stepped motor to synthesize the measurement aperture.

More details concerning the radar system can be found in [20].

A realistic scenario is considered with the radar system located very close to an external wall of the ground floor of one of the buildings of the faculty of engineering of the Second University of Naples. The wall has thickness equal to 0.24 m and dielectric permittivity of $4\epsilon_0$. The target to be imaged is a metallic circular cylinder having radius of 0.03 m located outside the building on the opposite side of the wall (see Fig. 4 for a pictorial view of the scene). The data are collected along a line at 0.74 m from the floor and the same configuration parameters as reported in Table 1 are adopted expect for the frequency step, which is now of 25 MHz, and for the investigation domain which is

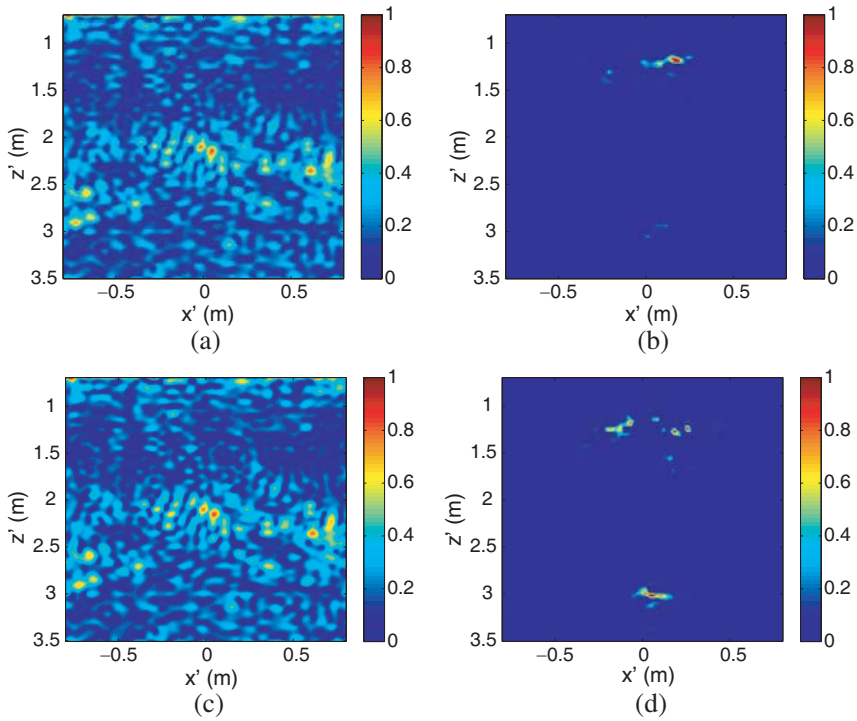

Figure 5. Normalized TSVD tomographic reconstructions and outcomes of the change detection procedure. (a) $|\mathcal{R}\chi_1|$. (b) $|\mathcal{R}\chi_1| - |\mathcal{R}\chi_2|$. (c) $|\mathcal{R}\chi_2|$. (d) $|\mathcal{R}\chi_2| - |\mathcal{R}\chi_1|$.

$D = [-0.8, 0.8] \times [0.7, 3.5]\,\mathrm{m}^2$.

We consider only two configurations:

$m = 1$, the target center is at about $(0.3, 1.2)$ m

$m = 2$, the target center is at about $(0.17, 3)$ m.

No further scatterers are present within the investigation domain so that the clutter arises from errors in modelling the wall. In particular, to emphasize this point, the reconstructions are obtained by adopting the total scattered field (i.e., the field reflected by the wall plus the one scattered by the target behind it).

The reconstructions corresponding to the two cases mentioned above are reported in panels (a) and (c) of Fig. 5. As can be seen, they look very similar and no information about the scatterers can be deduced. More in detail, as we known the wall parameters, a part from the wall contribution which would be manifested as two line due to the two interfaces, we expected the target being localized [7]. Instead, in both cases the target is very hard to be detected. This is due to a steel reinforcing grid present within the wall we completely neglected in the model and which obscures the scatterers located beyond it. Amazingly, the change detection procedure dramatically increases the detectability of the scatterers (see panels (b) and (d)) even though some spurious artifacts still remain for the more deeply located scatterer. The residual ambiguity is related to the fact that the case presented is very challenging. In fact, the more deeply located scatterer, due to its small cross section and a significant distance from the antennas compared to that of the steel grid, is imaged with an equivalent contrast function comparable with the artifacts arising by the difference between the images.

5. CONCLUSIONS

A simple procedure to detect change in a TWI scenario has been presented and validated against synthetic as well as experimental data. The relative simplicity of the proposed approach is in order to tackle the problem in realistic cases where the fastness and the reliability of the procedure are among the main requirements. Provided to have a slowly moving target the procedure proven to be effective in increasing the target detectability against clutter due to static scatterers. Moreover, it has been shown that the clutter arising from model errors in the wall modelling can be mitigated as well. As future development, we plan to address the evaluation of performance measures to better locate the proposed approach in the framework of the relevant literature.

ACKNOWLEDGMENT

Effort sponsored by the Air Force Office of Scientific Research, Air Force Material Command, USAF, under the grant number FA8655-08-1-3055. The U.S. Government is authorized to reproduce and distribute reprints for Governmental purpose notwithstanding any copyright notation thereon.

REFERENCES

1. Ferris, D. D. and N. C. Currie, "A survey of current technologies for through-wall-surveillance (TWS)," *Proceedings of SPIE*, Vol. 3577, 62–72, 1999.
2. Baranoski, E. J., "Through-wall imaging: Historical perspective and future directions," *J. Frank. Inst.*, Vol. 345, 556–569, 2008.
3. Soldovieri, F., R. Solimene, A. Brancaccio, and R. Pierri, "Localization of the interfaces of a slab hidden behind a wall," *IEEE Trans. Geosci. Remot. Sens.*, Vol. 45, 2471–2482, 2007.
4. Withington, P., H. Fuhler, and S. Nag, "Enhanching homeland security with advanced UWB sensors," *IEEE Microw. Mag.*, Vol. 4, 51–58, 2003.
5. Yang, Y. and A. E. Fathy, "See-through-wall imaging using ultra wideband short-pulse radar system," *IEEE Antennas and Propagation Society International Symposium*, 334–337, 2005.
6. Ahmad, F., M. G. Amin, and S. A. Kassam, "Syntethic aperture beamformer for imaging through a dielectric wall," *IEEE Trans. Aerosp. Electr. Systm.*, Vol. 41, 271–283, 2005.
7. Dehmollaian, M. and K. Sarabandi, "Refocusing through building walls using synthetic aperture radar," *IEEE Trans. Geosc. Rem. Sens.*, Vol. 46, 1589–1599, 2008.
8. Song, L. P., C. Yu, and Q. H. Liu, "Through-wall imaging (TWI) by radar: 2-D tomographic results and analyses," *IEEE Trans. Geosci. Remot. Sens.*, Vol. 43, 2793–2798, 2005.
9. Soldovieri, F. and R. Solimene, "Through-wall imaging via a linear inverse scattering algorithm," *IEEE Geosc. Rem. Sens. Lett.*, Vol. 4, 513–517, 2007.
10. Solimene, R., F. Soldovieri, G. Prisco, and R. Pierri, "Three-dimensional through-wall imaging under ambiguous wall parameters," in print on *IEEE Trans. Geosci. Remot. Sens.*
11. Ahamd, F., M. G. Amin, and G. Mandapati, "Autofocusing of through-the-wall radar imagery under unknown wall characterisitics," *IEEE Trans. Imag. Process.*, Vol. 16, 1785–1795, 2007.

12. Moulton, J., S. Kassam, F. Ahmad, M. Amin, and K. Yemelyanov, "Target and change detection in synthetic aperture radar sensing of urban structures," *Proceedings of the IEEE Radar Conference (RADAR'08)*, 2008.
13. Chew, W. C., *Waves and Fields in Inhomogeneous Media*, IEEE Press, Piscataway, NJ, 1995.
14. Bertero, M. and P. Boccacci, *Introduction to Inverse Problems in Imaging*, Institute of Physics, Bristol, UK, 1998.
15. Levanon, N., *Radar Principles*, Wiley, New York, 1988.
16. Potin, D., E. Duflos, and P. Vanheeghe, "Landamines ground-penetrating radar signal enhancement by digital filtering," *IEEE Trans. Geosci. Remot. Sens.*, Vol. 44, 2393–2406, 2006.
17. Li, J. and E. G. Zelnio, "Target detection with synthetic aperture radar," *IEEE Trans. Aerosp. Electr. Syst.*, Vol. 32, 613–627, 1996.
18. Giannopoulos, A., "GprMax2D/3D, Users Guide," www.gprmax.-org, 2002.
19. Soldovieri, F., R. Solimene, and G. Prisco, "A multiarray tomographic approach for through-wall imaging," *IEEE Trans. Geosci. Remot. Sens.*, Vol. 46, 1192–1199, 2008.
20. Parrini, F., M. Fratini, M. Pieraccini, C. Atzeni, G. De Pasquale, P. Ruggiero, F. Soldovieri, and A. Brancaccio, "ULTRA: Wideband ground penetrating radar," *Proc. of European Radar Conference EURAD 2006*, Manchester, UK, Sep. 2006.